ACCOUNTS of chemical research

Article

Cite This: Acc. Chem. Res. 2018, 51, 2672−2680

pubs.acs.org/accounts

Using Chemical Pumps and Motors To Design Flows for Directed Particle Assembly

Published as part of the Accounts of Chemical Research special issue "Fundamental Aspects of Self-Powered Nano- and Micromotors".

Oleg E. Shklyaev,[†] Henry Shum,[‡] and Anna C. Balazs*[,†]

[†]Department of Chemical Engineering, University of Pittsburgh, Pittsburgh, Pennsylvania 15261, United States

[‡]Department of Applied Mathematics, University of Waterloo, Waterloo, ON N2L 3G1, Canada

CONSPECTUS: Mechanical and electrical pumps are conventionally used to drive fluid flow in microfluidic devices; these pumps require external power supplies, thus limiting the portability of the devices. Harnessing catalytic reactions in solution allows pumping to be shifted into the chemical realm and alleviates the need for extraneous equipment. Chemical "pumps" involve surface-bound catalytic patches that decompose dissolved reagents into the products of the reaction. The catalytic reactions thereby produce chemical gradients that in turn generate pronounced flow fields. Such chemically-generated flows can be harnessed to transport particles in the solution and regulate their self-organization into complex structures within confined chambers. The challenge, however, is determining the reactions and conditions that will yield "programmable" flows, which permit control over the structure formation. In this Account, we review our modeling efforts to design chemical pumps (and "motors") to regulate the motion and assembly of microscopic particles in solution. In the first scenario, microcapsules release reagents in a microchamber with stationary catalytic patches and thereby act as "fuel" for the microcapsules' self-sustained motion. As the reagent is consumed, the capsules aggregate into "colonies" on the catalyst-covered sites. The shape of the assembled colonies can be tailored by patterning the distribution of the catalyst on the surface. Hence, these chemical pumps can be utilized to regulate the autonomous motion and targeted delivery of microcarriers in microfluidic devices. Notably, this fundamental physicochemical mechanism could have played a role in the self-organization of early biological cells (protocells). In the second example, the catalysts are localized on mobile, active particles, which are called "motors". Reactants dispersed in the solution are decomposed at the surface of the motors and produce a convective flow that transports both the active particles and nearby passive, non-coated particles. Depending on the numbers of active and passive particles and the structure of the self-organized cluster, these assemblies can translate or spin and thus act as self-assembled "conveyor belts" or gears in the microchamber. The latter examples involve the formation of two-dimensional structures. In the final scenario, we devise a mechanism for assembling three-dimensional towerlike structures using microcapsules in solution. Here, chemicals diffusing from a central patch on a surface generate a radially directed flow along the surface toward the center. This toroidal roll of fluid lifts the capsules above the patch and draws out the cluster into a tower, whose structure can be tailored by varying the attractive capsule−capsule and capsule−surface interaction strengths. Hence, our method of flow-directed assembly can permit the growth of reconfigurable 3D structures from simple subunits. Taken together, these findings facilitate the fabrication of stand-alone microfluidic devices that autonomously perform multistage chemical reactions and assays for portable biomedical applications and act as small-scale factories to autonomously build microscale components.

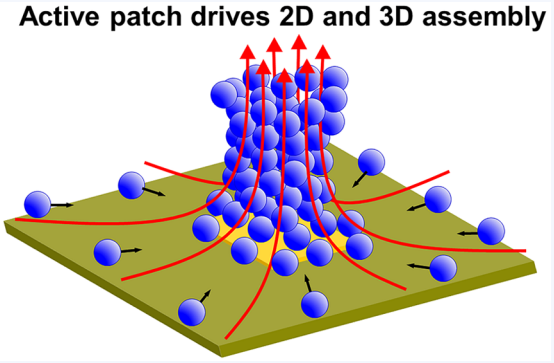

I. INTRODUCTION

Grinding and mixing of chemicals led to the early development of paints, which enabled humans to decorate solid "canvases" ranging from walls to utensils. There is a growing effort to extend the "canvas" to a fluid medium and use chemicals to effectively "paint" the fluid with spatiotemporal flow patterns, which could be used to regulate the collective behavior and dynamic self-organization of particles in solution. "Chemical pumps"[1] are providing a new method to achieve this level of control over flow fields. These "pumps" harness reactions in solution to generate gradients of chemical concentrations and fluid densities; in turn, these gradients give rise to net flows. The critical challenge is to design a palette of chemical reactions and scenarios that will lead to "programmable" flow fields. In essence, the goal is to move "pumping" from the mechanical and electrical realms to the chemical realm and

Received: May 28, 2018
Published: October 16, 2018

DOI: 10.1021/acs.accounts.8b00234
Acc. Chem. Res. 2018, 51, 2672−2680

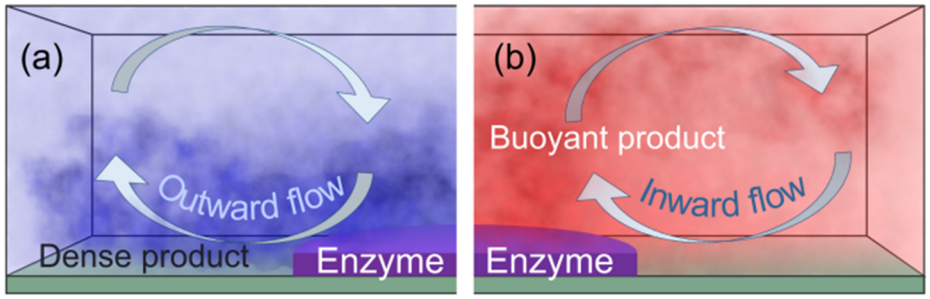

Figure 1. Outward and inward fluid flows induced by enzymatic (catalytic) reactions in solution.

thus enable new, chemically driven forms of self-powered particle transport and assembly.[2−7]

In this Account, we review our modeling efforts to design chemical systems that utilize solutal buoyancy effects[2−6] and diffusioosmosis[7] to regulate the motion and assembly of microscopic particles in solution. (We emphasize that this is not a comprehensive review but rather reflects our approaches to devise chemical pumps that controllably transport suspended particulates.) Both the solutal buoyancy and diffusioosmosis mechanisms produce chemical gradients that generate fluid flow. Since the two mechanisms can potentially be operative at the same time, it is important to understand whether one mechanism is dominant or if both are playing a significant role in the system's behavior. Below we describe the defining characteristics of each mechanism.

The phenomenon of solutal buoyancy[5] is illustrated in Figure 1, where a patch of enzyme (or other catalyst) in a microchamber interacts with reactants in solution, thereby generating a product that diffuses into the fluid. This reaction lowers the reactant concentration and raises the product concentration near the patch. The spatial distributions of the reactant and product introduce density variations $\Delta\rho$ that drive the spontaneous motion of the fluid through the buoyancy force $\mathbf{f}^{B} = \mathbf{g}\Delta\rho$, where $\mathbf{g}$ is the gravitational acceleration vector. Thus, the reaction acts as a chemical "pump" that propels the fluid. In a confined chamber, the continuity of the fluid will give rise to circular convective motion. If the products are denser than the reactants, then the product-rich fluid flows outward, away from the patch (Figure 1a); this in turn draws fresh, substrate-rich fluid from above toward the reactive patch. Conversely, if the products are less dense than the reactants, the fluid rises upward and thus draws fresh fluid inward toward the patch (Figure 1b). Importantly, because the catalytic patches react only with specific reagents, these systems combine sensing and fluidic pumping into a single self-powered microdevice.[1,8] While the flow velocities generated by these devices are a function of the catalytic turnover rate, velocities of up to 10 μm/s have been reported.[1]

Diffusioosmosis produces chemical gradients that generate fluid flow along a surface and acts as an independent pumping mechanism.[7,9−11] Diffusioosmosis arises from the interaction between solutes and solid surfaces in contact with the solution. In electrolyte solutions, for example, most surfaces acquire a net electric charge, and oppositely charged ions in the solution accumulate in a thin layer close to the surface. Additionally, if there is a gradient in the electrolyte concentration along the surface, then there will also be an induced electric field due to differences in the diffusion coefficients of the positive and negative ions of the electrolyte. The induced electric field acts on the charged layer of fluid near the surface, driving tangential fluid flow that can be approximated as $\mathbf{u}^{DO} = \gamma\left(\frac{\nabla_{\|} C}{C}\right)$, where $\nabla_{\|}C$ denotes the component of the concentration gradient parallel to the wall and γ is a functional that contains details of the intermolecular interactions between the solute molecules and the adjacent fluid−solid interfaces.[12] A simple and efficient way to model diffusioosmosis is to introduce a force $\mathbf{f}^{DO} \propto \mathbf{u}^{DO}$; with this force term, the diffusioosmotic and solutal buoyancy effects can be described in a similar manner.[7]

The differences between the two mechanisms for fluid motion can be explained as follows. Diffusioosmosis is an interfacial effect, where the solution at the fluid−solid interface is driven with a tangential velocity $\mathbf{u}^{DO}$. On the other hand, solutal buoyancy is a bulk effect where the driving force $\mathbf{f}^{B}$ is distributed throughout the volume occupied by the solution. In the absence of other mechanisms for fluid motion, the velocities generated by diffusioosmosis remain restricted by the boundary values $\mathbf{u}^{DO}$, which are defined by the details of the solution−wall interactions (characterized by γ). The velocities of buoyancy-driven flows, however, increase with the size of the fluidic system (i.e., the dimension parallel to $\mathbf{g}$). Therefore, for smaller systems (with a characteristic size of ∼0.1 mm)[13] the diffusioosmotic mechanism can dominate over the buoyancy effects, while for larger systems (on the order of 1 mm)[6] buoyancy effects can play the dominant role.

One way to distinguish between the diffusiophoretic/osmotic flow and density-driven pumping mechanisms described above is to invert the pump.[1] This inversion results in a reversal of the flow direction for the density-driven buoyancy mechanism but not for gravity-independent diffusiophoretic/osmotic flow. In both of these mechanisms, chemical reactions generate the spatiotemporal flow patterns that can transport nano- and microscopic particles.

Below we give a brief general summary of our modeling approaches,[2−7] which involve numerical solution of the coupled governing equations for the flowing incompressible fluid, dissolved reactive chemicals, and advected microscopic particles. We then describe specific findings where chemical reactions in the fluid gave rise to flows that enabled the directed transport of the suspended particles. The first two cases involve buoyancy-driven flow. In particular, we describe a form of "communication" between reagent-laden microcapsules in solution and catalyst-decorated surfaces.[3] When the reagents diffuse out of the porous capsules, they react with the immobilized catalytic sites and thereby generate the buoyancy-driven flows that carry the suspended microcapsules and drive them to aggregate into "colonies". The assembled colonies can be tailored by patterning the distribution of catalysts on the underlying surface.

DOI: 10.1021/acs.accounts.8b00234
Acc. Chem. Res. 2018, 51, 2672−2680

We also examine the behavior of enzyme-coated capsules placed on the bottom of a microchannel filled with dissolved reagent.[4] Fluid flow arising from the catalytic reaction on the coated capsules drives these spheres to move, and hence, we refer to the motile particles as chemical "motors". We combine these motors with passive, noncatalytic particles to prompt the collective motion of both the active and passives spheres.

Finally, in the third example, we drive the dynamic self-organization of spherical microparticles into three-dimensional (3D) vertical assemblies via diffusioosmotic flows generated by release of chemicals from a reservoir on the surface.[7] Our studies reveal that the concentration gradient of the diffusing species causes radially directed diffusioosmotic flow along the surface toward a central point. This flow drives the organization of the particles as these spheres push each other upward and form vertically oriented towers.

II. MODELING APPROACH

The behavior of dissolved chemicals and fluids moving with velocity $\mathbf{u} = (u_x, u_y, u_z)$ at pressure p can be described by equations for the following: the continuity of the fluid, the fluid dynamics (as given by the Navier–Stokes expression in the Boussinesq approximation[14]), and the diffusion of reagents in the solution.[3] The respective equations are

$$\nabla\cdot\mathbf{u} = 0 \tag{1}$$

$$\frac{\partial \mathbf{u}}{\partial t} + (\mathbf{u}\cdot\nabla)\mathbf{u} = -\frac{1}{\rho_0}\nabla p + \nu\nabla^2\mathbf{u} + \frac{1}{\rho_0}\mathbf{f}^{\mathrm{B}} + \frac{1}{\rho_0}\mathbf{f}^{\mathrm{DO}} \tag{2}$$

$$\frac{\partial C^j}{\partial t} + (\mathbf{u}\cdot\nabla)C^j = D^j\nabla^2 C^j + Q^j \tag{3}$$

Here we consider scenarios where either $\mathbf{f}^{\mathrm{B}}$ or $\mathbf{f}^{\mathrm{DO}}$ is equal to zero, so that one mechanism controls the fluid flow. The variable C^j characterizes the concentration of chemical j in the solution. Additionally, ∇ is the spatial gradient operator, ν is the kinematic viscosity, D^j is the diffusivity of reactant j, and Q^j is the corresponding source term describing the production or decomposition of chemicals during the chemical reactions. These equations are solved numerically[2−7] using the lattice Boltzmann method (LBM)[15−17] for the fluid dynamics.

In our previous studies,[5] we focused on convective flows that are dominated by solutal buoyancy effects, and thus, we ignored the relatively minor contributions from thermal buoyancy. Hence, variations in the density of the aqueous solution, $\Delta\rho$, depend on the concentrations C^j of N^C solute species measured relative to the corresponding reference values C_0^j $(1 \le j \le N^C)$:[18]

$$\Delta\rho = \rho_0 \sum_{j=1}^{N^C} \beta_C^j (C^j - C_0^j) \tag{4}$$

The volumetric solutal expansion coefficients β_C^j characterize the magnitudes of the density variations in response to changes in solute concentrations $C^j - C_0^j$.

Catalytic reactions occurring at surfaces coated with enzymes were modeled[2−6] using the Michaelis–Menten reaction rates

$$r^j = \frac{r_{\max} C^j}{K_{\mathrm{M}} + C^j} = Q^j \tag{5}$$

where the maximal reaction rate $r_{\max} = k_{\mathrm{cat}}[\mathrm{E}]$ incorporates the reaction rate per molecule of enzyme k_{cat} and the enzyme concentration $[\mathrm{E}]$ and K_{M} is the Michaelis constant.

III. CONVECTION-DRIVEN AGGREGATION OF LEAKY MICROCAPSULES

To achieve the first example of "programmable" flows and directed self-organization, we focus on porous microcapsules (with radii in the range $R = 10-50$ μm) that release hydrogen peroxide into a fluid-filled microchamber containing a patch of the enzyme catalase on the bottom wall.[3] The encapsulated H_2O_2 diffuses out of these microcarriers at the rate $\frac{4\pi R^3}{3}Q = -\frac{\mathrm{d}M}{\mathrm{d}t} = \frac{3P}{R}M_0\exp(-3Pt/R)$, where $P = D_{\mathrm{in}}/d$ is the permeability of the microcapsule's shell and $M = C_{\mathrm{in}}4\pi R^3/3$ is the amount of the encapsulated reagents, given an initial value M_0.

The following reaction occurs when the released reagents interact with the enzymes: $2H_2O_2 \xrightarrow{\text{catalyst}} 2H_2O + O_2$. Because the products are less dense than the reactants, the reaction generates an inward flow that transports the sedimenting capsules toward the enzyme-coated patch. As demonstrated below, the capsules organize into clusters that reproduce the shape of the patch and remain in this configuration after the reagent is depleted from the system.

We simulated the dynamics of N capsules in a rectangular domain with height $H = 1$ mm and equal horizontal sizes $L = 4$ mm (Figure 2). The condition requiring zero velocities ($\mathbf{u} = \mathbf{0}$) for the fluid and zero chemical fluxes were imposed over the top and bottom solid boundaries and periodic boundary conditions were enforced at the side walls of the simulation box. Initially, the capsules were uniformly dispersed in the water-filled domain, and each capsule contained a 30% hydrogen peroxide solution ($C_0 = 14$ M). As the capsules sediment, they release the reactants, which interact with the enzyme-coated patch. As a result of the chemically generated inward flow, the capsules rise above the patch and, by the fluid continuity, are carried toward the patch along the bottom wall. The arrows in Figure 3 show the local fluid velocity with the maximal value achieved above the center of the enzyme-covered patch (indicated in blue in the images on the right).

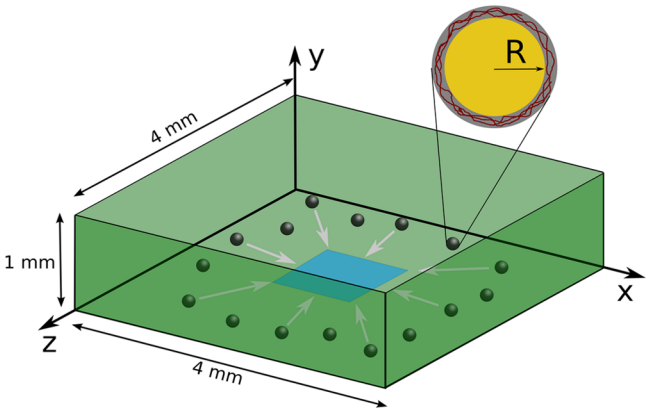

Figure 2. Enzyme (blue square) catalyzes the decomposition of the reagent, which generates an upward flow above the patch. The flow draws capsules toward the patch. The structure of a capsule with a polymer shell and core region of radius R containing the reagent is shown in the inset.

DOI: 10.1021/acs.accounts.8b00234
Acc. Chem. Res. 2018, 51, 2672−2680

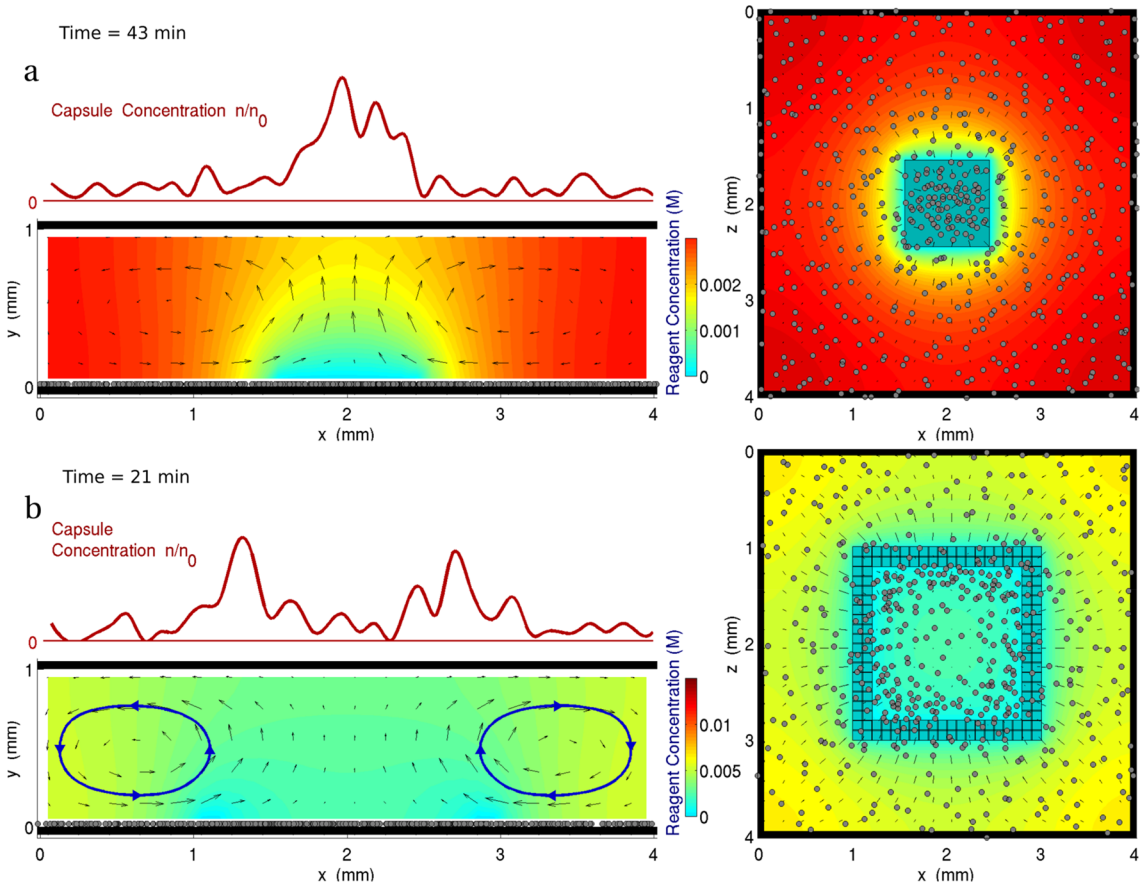

Figure 3. (a) Convective aggregation of $N = 500$ capsules with radius $R = 15$ μm and shell permeability $P = 10^{-6}$ m/s above the square enzyme-coated patch (blue square in the right panel). (b) Convective aggregation of $N = 500$ capsules with radius $R = 20$ μm and shell permeability $P = 10^{-6}$m/s above an enzyme patch in the form of a hollow square. Colors ranging from red (fuel-rich) to blue (fuel-depleted) indicate the hydrogen peroxide concentration, which varies from 0 to 0.003 M. Arrows show the direction of the fluid flow. The relative densities of the capsules n/n_0 (illustrating aggregation) are shown with red lines above the images in the left panels.

The aggregation of capsules can be quantified by their areal concentration $n = m/A'$, defined as the number of capsules m located within a square region of area $A' = 0.4$ mm $\times$ 0.4 mm centered at position (x, z) on the bottom surface. Normalized by the initial uniform distribution $n_0 = N/L^2$, the values of the capsule concentration n/n_0 are shown with a red line in the left panel in Figure 3a. The peaks in n/n_0 approximately coincide with the position of the enzyme-coated patches. (The arrows in the underlying figures clearly show that the fluid flows upward above the patch.) After all of the reagent is consumed, the fluid motion stops, and capsules remain in colonies, approximately reproducing the configuration of the patch.

The shape of the enzyme-coated patch generating the convective flow can promote the self-assembly of capsules into structured clusters. An example of a cluster aggregated on a patch that forms a hollow square is shown in Figure 3b. Different amounts of the fuel within the capsules allow groups of capsules with different radii to form clusters with different configurations in response to the flow generated by the same patch. For example, a group consisting of $N = 1000$ small capsules with radius $R = 15$ μm aggregate into colonies approximately reproducing the shapes of the enzyme patches in Figure 4a,b. On the other hand, Figure 4c,d shows that groups consisting of $N = 500$ large capsules with radius $R = 40$ μm assemble into colonies with a completely filled interior, despite the hollow shapes of the enzyme-coated patches generating the convection.

The observed differences in the final cluster configurations are due to differences in the convective regimes that transport the capsules; these regimes are characterized by the velocities and structures of the flows. In particular, the simulations revealed that capsules with a larger radius R can reach higher rates of aggregation for the following reasons. First, the larger capsules contain a greater amount of the fuel, which can generate faster fluid flows. Second, spherical capsules with larger surface areas experience larger fluid drag because the fluid velocity near the wall increases almost linearly from a value of zero at the wall. The capsules with larger radii thus experience larger values of the velocity. The faster flows can aggregate capsules into denser clusters, with the final structure limited by the formation of the close-packed monolayer. (The flows near the bottom surface are sufficiently slow that all of the assembled clusters are two-dimensional.)

In this example, fluid motion was driven by a chemical pump that was immobilized on the bottom wall. If the enzyme is instead coated onto the surface of a motile particle, then this particle becomes a chemical "motor", as described in the following section.

DOI: 10.1021/acs.accounts.8b00234
Acc. Chem. Res. 2018, 51, 2672−2680

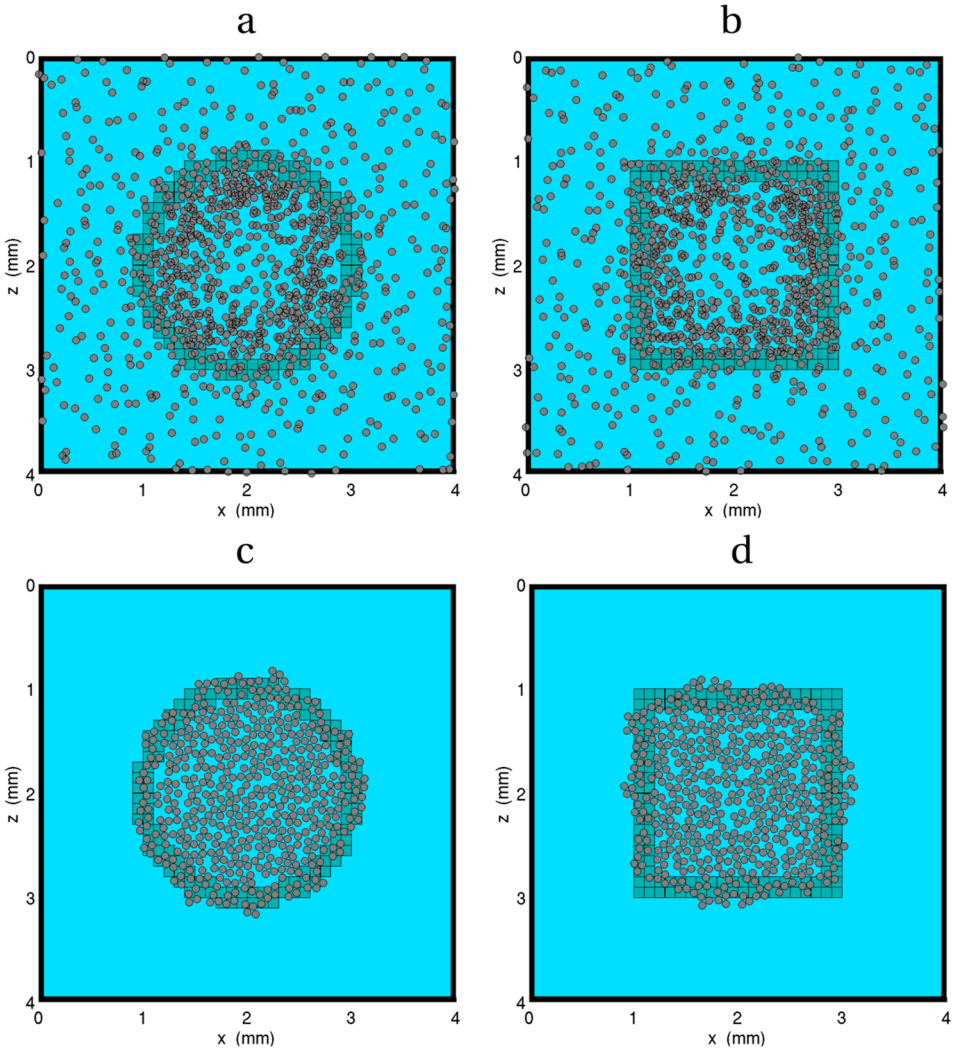

Figure 4. Colonies of capsules assembled above enzyme-coated patches with different shapes. (a, b) Aggregation of $N = 1000$ capsules with radius $R = 15$ above enzyme-coated patches in the form of (a) a hollow circle and (b) a hollow square. (c, d) Aggregation of $N = 500$ capsules with radius $R = 40$ μm above (c) a hollow circle and (d) a hollow square. The snapshots show the final positions of the capsules after the all of the reagent in the system is depleted and the fluid has motion stopped. The capsules are indicated by the gray dots, which are not drawn to scale.

IV. SELF-AGGREGATION OF MOTORS AND PASSIVE PARTICLES

Chemical pumps that are not stationary but can move in the fluid are called "motors". Here the motor is a microscopic particle that is uniformly coated with the enzyme catalase that decomposes hydrogen peroxide, which is initially uniformly distributed in the solution.[4] (The initial hydrogen peroxide concentration is set to be 1 M.) We also introduce passive particles, which are not coated with the enzyme. Both types of particles are denser than the solution and thus sediment to the bottom of the domain. (We set the particle density to $\rho_C = 1.1\rho_0$, where ρ_0 is the density of water.) The dynamics of the system are described by eqs 1−3, with the chemical sources, Q, localized at the surfaces of the active particles. Periodic boundary conditions for the fluid velocities and chemicals were imposed on the side walls of the 3D simulation box.

We first considered the case involving two particles,[4] one active (shown in red in Figure 5) and one passive (shown in blue). The reactants in solution are decomposed into the less dense products by the catalysts on the surface of the active particle. The resulting flow rises above the active particle and forms vortexes that drag the passive sphere toward the active one (Figure 5a) until the particles form a dimer. The drag force imposed by the fluid and directed from the passive particle to the active particle enables translation of the dimer along the bottom wall (Figure 5b,c).

The depletion of the reactants in the domain (as indicated by the progressively lighter colors in the sequential panels in Figure 5) fuels the propulsion of these particles. The panels also show that the upward flow generated by the active particle translates with the moving particle, revealing a coupling between the particle positions $\mathbf{r}_i$ and the flow $\mathbf{u}(\mathbf{r}_i)$.

Multiple particles interacting via the fluid flow can assemble into a cluster that is defined by the particle coordinates and coupled to the self-consistent global flow, which is generated by the cluster and defines its structure. The dynamics of such a self-propelled cluster depends on the geometry of the channel, the properties of the particles, the configuration of the clusters of particles, and the chemical reaction used to generate the fluid motion.

In the case of multiple particles, this self-consistent behavior can lead to distinctive forms of convective self-organization. To

DOI: 10.1021/acs.accounts.8b00234
Acc. Chem. Res. 2018, 51, 2672−2680

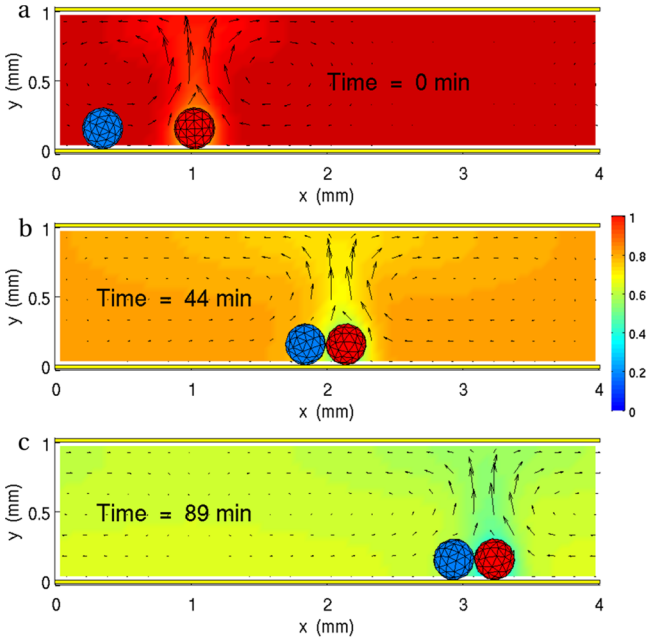

Figure 5. Side view of a 3D simulation domain showing (a) dimer formation and (b, c) propulsion. Fluid flow (indicated by the arrows), generated by chemical decomposition of the reagent around a mobile active particle (red), drags a passive particle (blue), which transmits momentum to the active one and pushes the dimer to the right. Depletion of the reagent concentration (in units of M) fueling the reaction around the active particle is indicated by the color bar.

investigate the rich dynamics that can emerge in these systems, we considered clusters denoted as (N_a, N_p) that consist of N_a active (red) and N_p passive (blue) particles. The particle arrangement $\{\mathbf{r}_i, i = 1, 2, \cdots, N\}$, where $N = N_a + N_p$, gives rise to the generated fluid flow $\mathbf{u}(\{\mathbf{r}_i\})$. The cases described below exemplify how the relative number and arrangement of these spheres plays a crucial role in the evolution of the system. Namely, some initial configurations remain stable and translate as a cluster along the surface. Other configurations reorganize into stable structures that can then translate or even rotate. Notably, some configurations remain motionless.

In the ensuing simulations, particles were placed on the bottom plane. If an initially prescribed configuration of the cluster remained unchanged during the entire simulation, it was considered to be stable; if the configuration spontaneously reorganized into a different shape, it was taken to be metastable.

As a natural progression, we first considered the behavior of representative trimers. Figure 6 reveals how an initially metastable collinear trimer $(1_a, 2_p)$ transforms into a stable, motile triangular configuration (brown line). The green line shows the transition of an initially metastable stationary trimer $(2_a, 1_p)$ into a traveling triangular structure. The blue curve serves as a reference, indicating the motion of the dimer $(1_a, 1_p)$ discussed above.

The dynamical behavior of the system becomes more complex when the total number of particles within the simulation domain is greater than 3. The simulated cluster configurations[4] and the corresponding types of dynamics are summarized in Figure 7. The arrangements of active and passive particles that possess mirror symmetry enable the clusters to translate or remain stationary. Transformations of metastable clusters into stable clusters that are observed in the

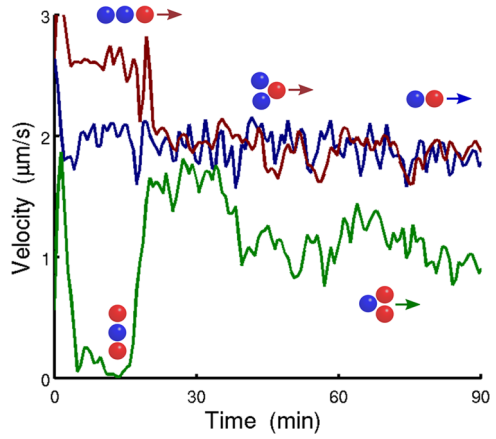

Figure 6. Average speed $|\sum_i^N \mathbf{u}_i|/N$ of clusters formed by N_a active (red) and N_p passive (blue) particles. The particle radius is R = 150 μm, and the reaction rate associated with each active particle is k_{max} = 0.003 mol s^{-1} m^{-2}. Arrows next to the insets show the directions of propulsion for the different clusters. Arrow colors match the corresponding velocity curves. Clusters without arrows are stationary.

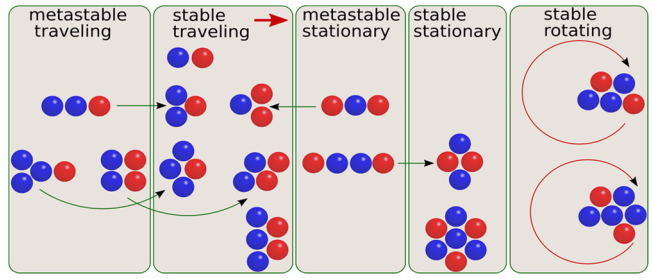

Figure 7. List of (N_a, N_p) clusters containing N_a active (red) and N_p passive (blue) particles, which show different behavior depending on the composition and particle arrangement. Transitions from metastable to stable isomers are shown with green arrows. Propulsion directions are shown with red arrows. Symmetric clusters are propellled or remain stationary, while asymmetric clusters rotate.

simulations are indicated by green arrows. The absence of mirror symmetry can result in rotation, as shown in Figure 6 for the $(2_a, 3_p)$ and $(2_a, 4_p)$ clusters that contain odd $(N = 5)$ and even $(N = 6)$ numbers of particles, respectively. The direction of rotation is indicated with red arrows.

Notably, the velocities of the dimer $(1_a, 1_p)$, trimer $(1_a, 2_p)$, and pentamer $(2_a, 3_p)$ differ by less than 3% (at time equal to 35 min),[4] indicating that the speed of propulsion does not scale with the number of active or passive particles. One reason for the limitation on the speed of the clusters is that interactions between active and passive particles are vector quantities. In the triangular trimer $(1_a, 2_p)$, for instance, the two passive particles push the active particle in different directions so the net motion is not simply twice as fast as that of the dimer $(1_a, 1_p)$. Furthermore, interactions between the passive particles themselves, as well as between just the active particles, must also be taken into account. The overall cluster motion, dictated by the balance of all of these interactions, is highly dependent on the arrangement of particles and does not necessarily speed up with the number of particles. This behavior also implies that particles can have different roles within the cluster: some are essential for the propulsion of the cluster, while others are the effective cargo.

DOI: 10.1021/acs.accounts.8b00234
Acc. Chem. Res. 2018, 51, 2672−2680

These findings show that active particles can be harnessed to autonomously transport a cargo of passive spheres in the microchamber. The ability to perform this operation does depend on the initial arrangement of the active "engine" and the load. Nonetheless, for a stable traveling system, the assembly will continue to move until the reactants in the solution are depleted.

V. TOWER FORMATION

Having demonstrated self-organization of particles into 2D assemblies, we then focused on approaches to drive the self-organization of microcapsules into three-dimensional towerlike structures.[7] To achieve this behavior, we designed a system in which a chemical is released from a catalytic patch on the bottom wall of a chamber. The resulting chemical concentration gradient along the surface induces diffusioosmotic flow, which is characterized by a tangential velocity $\mathbf{u}^{DO}$ that depends on the constant γ. We set γ to be positive so that flow is directed toward regions of higher concentration.

The computational grid size was $L \times H \times L$ with the horizontal length $L = 150$ and vertical height $H = 75$ in most simulations. We set the grid spacing to the physical length scale $\Delta x = 1$ μm. We prescribed periodic boundary conditions in the horizontal (x and z) directions and used zero fluid velocity ($\mathbf{u} = \mathbf{0}$) conditions on the lower and upper (y) walls. A force density $\mathbf{f}^{DO} \propto \mathbf{u}^{DO}$ was applied at lattice nodes adjacent to the bottom boundary to drive fluid motion.

Microcapsules in the fluid are advected by the flow and experience short-range attractive interactions with each other and with the wall (modeled by Morse potentials) that tend to stabilize clusters of particles. The motion of the microcapsules was coupled to the fluid flow using the immersed boundary (IB) method,[19−21] which approximately enforces the boundary condition that the fluid velocity at any point on the surface of a capsule is equal to the velocity of the capsule shell at that point.

We began each simulation with $N^{cap} = 60$ capsules randomly positioned on the bottom wall of the chamber ($y = 0$). The diffusioosmotic flow drives the motion of the fluid throughout the chamber, and the capsules are advected with the flow toward the catalytic patch.

The attractive interaction between the wall and the capsules prevents the capsules from detaching. Since our objective was to form a tower, however, we required the capsules to lift off from the surface once they reached the center of the patch. A circular region with no capsule−wall attraction was placed at the center of the catalytic patch. Capsules tend to aggregate around this nonattractive patch because they are driven inward by the diffusioosmotic flow, but there is an energy barrier at the boundary between the attractive and nonattractive regions of the wall. As more capsules aggregate at the patch, the inner capsules are pushed through the energy barrier and become detached from the wall. These wall-detached capsules, which remain attached to neighboring capsules, are then lifted up by the fluid flow and collectively form a towerlike structure. The overall process is shown schematically in Figure 8.

The formation of the tower involves a subtle interplay between the effects of the fluid flow (which drags the capsules) and the energetic interactions in the system. Namely, for robust tower formation, the strength of the capsule−wall attraction must be carefully controlled. In our simulations, we systematically varied the depths of the wells in the Morse potentials describing the capsule−surface and capsule−capsule attractions. Three representative simulations with the same capsule−capsule attraction are shown in Figure 9. When the depth of the potential well describing the capsule−surface attraction was relatively low, the capsules formed a large cluster that eventually detached from the wall (Figure 9a). At the intermediate value, capsules assembled into a tall tower (Figure 9b), whereas a small mound surrounded by a monolayer of aggregated capsules formed when the potential well was too deep (Figure 9c). The formation of towers therefore requires control of interparticle interactions, which can be achieved experimentally by functionalizing the surfaces of the capsules and adjusting the pH and ionic strength of the solution.[22]

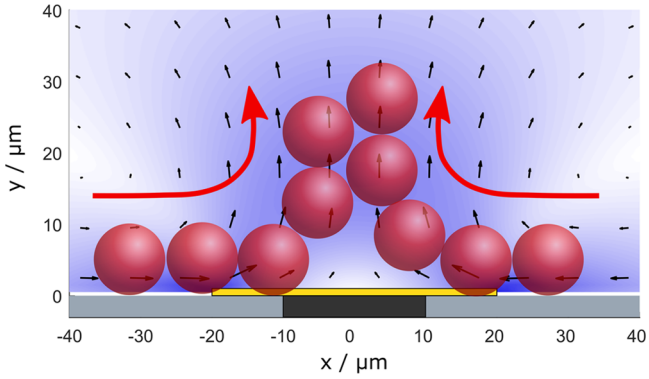

Figure 8. Towers of capsules assembled by diffusioosmotic flow. A chemical is produced and diffuses from the catalytic patch represented by the thin yellow strip on the bottom of the chamber. The fluid flow, driven by diffusioosmosis, is visualized by the small, black arrows. The relative magnitudes of flow speeds are indicated by the blue background shading; higher speeds are represented by deeper blue. Capsules move in the direction of the curved red arrows. Capsules initially travel along the attractive portion of the wall (light gray) but later detach at the nonattractive region (dark gray) and rise upward to form towerlike structures.

VI. CONCLUSIONS

Catalytic reactions in fluid-filled chambers play a crucial role in industrial processes and biological phenomena and possibly influenced the aggregation of the earliest biological cells. Only recently, however, have we begun to harness catalytic reactions to direct the movement and self-organization of particles in solution. The ability to regulate particle motion without significant external intervention is particularly important for improving the portability of microfluidic devices, allowing them to be used at the point of care. As shown above, when microcapsules that enclose reagents (and other cargo) are introduced into a microchamber decorated with catalytic patches, the system can utilize the reagents as the "fuel" for the microcapsules' self-sustained motion and enable the targeted delivery of microcarriers to specific sites in the device. Hence, the device could operate in an autonomous manner.

We also predicted that the flows generated with different arrangements of the anchored catalysts permit the capsules to be assembled into clusters of specified shapes. These predictions are supported by recent experiments[23] showing that convective flows in microchambers can drive the 2D assembly of particles into colloidal crystals of the desired structure and orientation.

The microcapsules considered here can serve as models for protocells, which resembled leaky, fluid-filled sacks that lacked complex biochemical machinery. It is unclear how protocells

DOI: 10.1021/acs.accounts.8b00234
Acc. Chem. Res. 2018, 51, 2672−2680

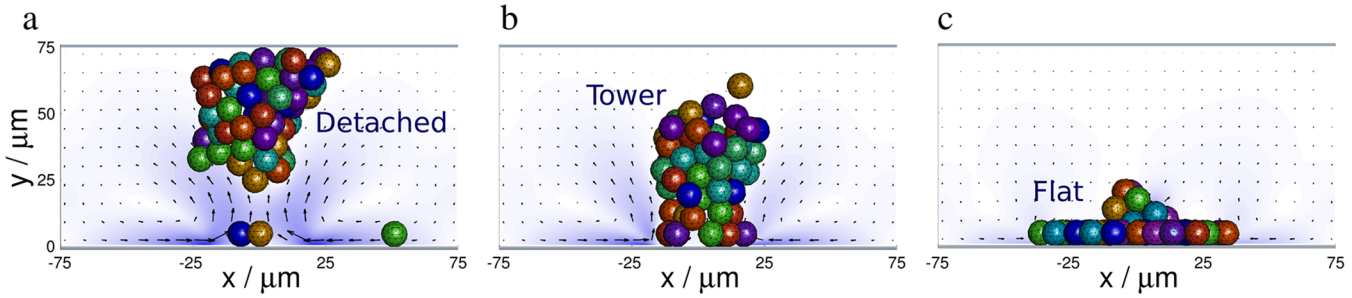

Figure 9. Outcomes of flow-driven aggregation of capsules as the depth of the capsule−wall potential well, A, is varied. Defining A_{mid} to be the depth of the potential well for capsule−surface attraction in the intermediate case, the parameter values in the three examples are (a) $A = 0.75A_{mid}$, (b) $A = A_{mid}$, and (c) $A = 2A_{mid}$. Towers form correctly only for an intermediate range of well depths (b). If the well is too shallow (a), then any cluster that forms detaches from the surface. If the well is too deep (c), capsules aggregate into flat clusters with most of the capsules remaining in contact with the wall.

communicated and self-organized into larger colonies. This level of self-organization was vital for the cells' chances of survival and ultimately the formation of differentiated structures such as organelles. Our findings suggest one possible mechanism: small chemicals diffusing from the porous protocells reacted with nearby mineral catalysts and thereby produced density-driven convective flows, which enabled the protocells to congregate on the surfaces, much as capsules in Figure 3a.

Synergetic interactions occurring in the fluid become particularly complex when the catalytic reaction occurs on the surface of a mobile particle, i.e., a "motor". Here, the fluid flow generated by the motor affects the motor's motion. Moreover, flow fields generated by buoyancy-driven motors can transport noncatalytic passive particles (cargo) in the solution. Cargo dragged by the fluid transmits momentum to the neighboring particles within the cluster and thereby affects the cluster's propulsion. Given this interconnected, dynamic behavior, modeling studies provide an effective tool to determine fundamental relationships between the numbers of active and passive particles and the structure, stability, and velocity of the evolving clusters. Our studies can facilitate the fabrication of self-propelled clusters with the appropriate geometry and dynamics to perform specific functions in microfluidic devices. For example, rotating clusters could serve as microgears within the chamber. It is noteworthy that recent experiments on platinum-coated colloids in solution revealed that the decomposition of hydrogen peroxide on the surface of these particles generated buoyancy-driven convective flows, which in turn advected the coated particles.[24] Hence, both our simulations and the experiments indicate that active particles could be used to tune mass transport in microfluidic devices.

Finally, we described a method for directing the assembly of spherical microcapsules into three-dimensional towerlike structures. The aggregation of the microcapsules is driven by diffusioosmotic flow along the surface toward a catalytic patch. Within a range of capsule−wall and capsule−capsule attractions, the structures grow upward as new capsules are inserted between the surface and the existing structure. The tower morphology can be controlled by patterning the shape of the surface-bound catalytic patches. Hence, these studies provide guidelines for utilizing microfluidic devices for the bottom-up assembly of complex 3D structures at specific locations.

The results also hint at the rich spatiotemporal phenomena that might be achieved by using cascades of chemical reactions. Such reaction networks could regulate the motion of the particles along specific paths at specific time intervals, much as traffic lights regulate the movement of vehicles. By achieving this level of regulation, researchers could fabricate stand-alone microfluidic devices that perform multistage chemical reactions and processes, such as autonomously shuttling particles and exchanging cargo between different regions as well as potentially performing logic operations.

As a specific example, the coupling of chemical cascades and chemical motors can lead to a particularly exciting research opportunity. (In the absence of chemical motors, researchers have used cascades of enzymatic reactions to generate buoyancy-driven flows with complex spatiotemporal patterns.[25]) If the product of a catalytic reaction on the surface of one chemical motor produces the reactant for another catalyst-coated particle, then the motion of these motors can become highly correlated and lead to novel forms of self-organization. This self-organization can be modulated by tailoring the reaction rates on the surfaces of the different motors (see eq 5). Hence, chemically coupled motors provide a new arena for designing colonies of synthetic particles that undergo correlated energy transduction, communication, and motion. By exploring this design space, researchers can devise chemically distinct motors that cooperate to perform complex tasks and thus establish a "toolkit" for fabricating self-powered, small-scale robotic systems that perform collaborative work. With the rapid developments of new chemical pumps[26] and motors,[27,28] we anticipate that control over the dynamic interplay between chemistry and fluid flow will enable new functionalities and technological applications.

AUTHOR INFORMATION

Corresponding Author

*E-mail: balazs@pitt.edu.

ORCID

Anna C. Balazs: 0000-0002-5555-2692

Notes

The authors declare no competing financial interest.

Biographies

Oleg E. Shklyaev received his Ph.D. from Institute of Continuous Media Mechanics, Russian Academy of Sciences. Currently he is a postdoctoral fellow at the University of Pittsburgh, where his research is focused on applications of chemically driven flows to manipulations with microparticles.

DOI: 10.1021/acs.accounts.8b00234
Acc. Chem. Res. 2018, 51, 2672−2680

Henry Shum is an Assistant Professor in the Department of Applied Mathematics at the University of Waterloo. He previously held postdoctoral positions at the University of Pittsburgh and the University of Oxford. His research areas include biolocomotion, fluid−structure interactions, and electrokinetic effects in low Reynolds number flows.

Anna C. Balazs is the Distinguished Professor of Chemical Engineering and holds the John A. Swanson Endowed Chair in Engineering at the University of Pittsburgh. She received her B.A. in physics from Bryn Mawr College and her Ph.D. in materials science from the Massachusetts Institute of Technology. Her research involves developing theoretical and computational models to capture the behavior of polymeric materials, nanocomposites, and multicomponent fluids.

■ ACKNOWLEDGMENTS

A.C.B. acknowledges the NSF for funding (Grant 1740630, CCI Phase I: Center for Chemomechanical Assembly) and the Center for Research Computing at the University of Pittsburgh for computer time.

■ REFERENCES

(1) Sengupta, S.; Patra, D.; Ortiz-Rivera, I.; Agrawal, A.; Shklyaev, S.; Dey, K. K.; Córdova-Figueroa, U.; Mallouk, T. E.; Sen, A. Self-Powered Enzyme Micropumps. *Nat. Chem.* **2014**, *6*, 415−422.
(2) Ortiz-Rivera, I.; Shum, H.; Agrawal, A.; Sen, A.; Balazs, A. C. Convective Flow Reversal in Self-powered Enzyme Micropumps. *Proc. Natl. Acad. Sci. U. S. A.* **2016**, *113*, 2585−2590.
(3) Shklyaev, O. E.; Shum, H.; Sen, A.; Balazs, A. C. Harnessing surface-bound enzymatic reactions to organize microcapsules in solution. *Sci. Adv.* **2016**, *2*, e1501835.
(4) Shklyaev, O. E.; Shum, H.; Yashin, V. V.; Balazs, A. C. Convective self-sustained motion in mixtures of chemically active and passive particles. *Langmuir* **2017**, *33*, 7873−7880.
(5) Valdez, L.; Shum, H.; Ortiz-Rivera, I.; Balazs, A. C.; Sen, A. Solutal and Thermal Buoyancy Effects in Self-Powered Phosphatase Micropumps. *Soft Matter* **2017**, *13*, 2800−2807.
(6) Das, S.; Shklyaev, O. E.; Altemose, A.; Shum, H.; Ortiz-Rivera, I.; Valdez, L.; Mallouk, T. E.; Balazs, A. C.; Sen, A. Harnessing Catalytic Pumps for Controllable Delivery of Microparticles in Microchambers. *Nat. Commun.* **2017**, *8*, 14384.
(7) Shum, H.; Balazs, A. C. Flow-driven Assembly of Microcapsules into Three-dimensional Towers. *Langmuir* **2018**, *34*, 2890−2899.
(8) Ortiz-Rivera, I.; Courtney, T. M.; Sen, A. Enzyme Micropump-Based Inhibitor Assays. *Adv. Funct. Mater.* **2016**, *26*, 2135−2142.
(9) Kline, T. R.; Paxton, W. F.; Wang, Y.; Velegol, D.; Mallouk, T. E.; Sen, A. Catalytic Micropumps: Microscopic Convective Fluid Flow and Pattern Formation. *J. Am. Chem. Soc.* **2005**, *127*, 17150−17151.
(10) Yadav, V.; Zhang, H.; Pavlick, R.; Sen, A. Triggered "On/Off" Micropumps and Colloidal Photodiode. *J. Am. Chem. Soc.* **2012**, *134*, 15688−15691.
(11) McDermott, J. J.; Kar, A.; Daher, M.; Klara, S.; Wang, G.; Sen, A.; Velegol, D. Self-Generated Diffusioosmotic Flows from Calcium Carbonate Micropumps. *Langmuir* **2012**, *28*, 15491−15497.
(12) Anderson, J. L. Colloid Transport by Interfacial Forces. *Annu. Rev. Fluid Mech.* **1989**, *21*, 61−99.
(13) Shin, S.; Um, E.; Sabass, B.; Ault, J. T.; Rahimi, M.; Warren, P. B.; Stone, H. A. Size-dependent Control of Colloid Transport Via Solute Gradients in Dead-end Channels. *Proc. Natl. Acad. Sci. U. S. A.* **2016**, *113*, 257−261.
(14) Chandrasekhar, S. *Hydrodynamic and Hydromagnetic Stability*; Clarendon Press: Oxford, U.K., 1961.
(15) Chen, S.; Doolen, G. D. Lattice Boltzmann Method for Fluid Flows. *Annu. Rev. Fluid Mech.* **1998**, *30*, 329−364.
(16) Ladd, A. J. C.; Verberg, R. Lattice-Boltzmann Simulations of Particle-Fluid Suspensions. *J. Stat. Phys.* **2001**, *104*, 1191−1251.
(17) Aidun, C. K.; Clausen, J. R. Lattice-Boltzmann Method for Complex Flows. *Annu. Rev. Fluid Mech.* **2010**, *42*, 439−472.
(18) Pojman, J. A.; Epstein, I. R. Convective Effects on Chemical Waves. 1. Mechanisms and Stability Criteria. *J. Phys. Chem.* **1990**, *94*, 4966−4972.
(19) Peskin, C. S. Numerical Analysis of Blood Flow in the Heart. *J. Comput. Phys.* **1977**, *25*, 220−252.
(20) Peskin, C. S. The Immersed Boundary Method. *Acta Numer.* **2002**, *11*, 479−517.
(21) Feng, Z.-G.; Michaelides, E. E. The Immersed Boundary-Lattice Boltzmann Method for Solving Fluid−particles Interaction Problems. *J. Comput. Phys.* **2004**, *195*, 602−628.
(22) Letteri, R. A.; Santa Chalarca, C. F.; Bai, Y.; Hayward, R. C.; Emrick, T. Forming Sticky Droplets from Slippery Polymer Zwitterions. *Adv. Mater.* **2017**, *29*, 1702921.
(23) Niu, R.; Palberg, T. Seedless Assembly of Colloidal Crystals by Inverted Micro-fluidic Pumping. *Soft Matter* **2018**, *14*, 3435−3442.
(24) Gregory, D. A.; Ebbens, S. J. Symmetrical Catalytically Active Colloids Collectively Induce Convective Flow. *Langmuir* **2018**, *34*, 4307−4313.
(25) Zhang, Y.; Tsitkov, S.; Hess, H. Complex Dynamics in a Two-enzyme Reaction Network With Substrate Competition. *Nature Catalysis* **2018**, *1*, 276−281.
(26) Zhou, C.; Zhang, H.; Li, Z.; Wang, W. Chemistry Pumps: a Review of Chemically Powered Micropumps. *Lab Chip* **2016**, *16*, 1797−1811.
(27) Dey, K. K.; Sen, A. Chemically Propelled Molecules and Machines. *J. Am. Chem. Soc.* **2017**, *139*, 7666−7676.
(28) Ebbens, S. *Curr. Opin. Colloid Interface Sci.* **2016**, *21*, 14−23.

DOI: 10.1021/acs.accounts.8b00234
Acc. Chem. Res. 2018, 51, 2672−2680